fluids

MDPI

Article

Dynamics of Magnetic Fluids and Bidisperse Magnetic Systems under Oscillatory Shear

Elena Shel'deshova, Alexander Churaev and Petr Ryapolov *

Faculty of Natural Sciences, Department of Nanotechnology, Microelectronics, General and Applied Physics, Southwest State University, 50 Let Oktyabrya Str. 94, Kursk 305040, Russia
* Correspondence: r-piter@yandex.ru

Abstract: This article presents the results of a study on the dynamics of a volume of magnetic fluid levitating in a uniform magnetic field of an electromagnet experiencing an oscillatory shift. Samples with different physical parameters were considered, and the dependence of the magnetoviscous effect was studied. It showed that the greatest influence on the dynamics of a magnetic fluid that experiences vibrational-shear and magnetic-viscosity effects is exerted by the sample microstructure and the presence of large magnetic particles. The results of this work can be used in the development of a technique for magnetic fluid samples express testing, as well as in the development of acceleration and vibration sensors based on magnetic fluids

Keywords: magnetic fluids; bidisperse magnetic systems; smart materials; magnetic field; oscillatory shift; magnetoviscous effect

check for updates

Citation: Shel'deshova, E.; Churaev, A.; Ryapolov, P. Dynamics of Magnetic Fluids and Bidisperse Magnetic Systems under Oscillatory Shear. *Fluids* **2023**, *8*, 47. https://doi.org/10.3390/fluids8020047

Academic Editors: Ahmed Rashad and Mehrdad Massoudi

Received: 9 December 2022
Revised: 29 December 2022
Accepted: 11 January 2023
Published: 28 January 2023

Copyright: © 2023 by the authors. Licensee MDPI, Basel, Switzerland. This article is an open access article distributed under the terms and conditions of the Creative Commons Attribution (CC BY) license (https://creativecommons.org/licenses/by/4.0/).

1. Introduction

Nanodispersed magnetic fluid (MF) is a colloidal system of magnetic nanoparticles with a size of 5 to 20 nanometers, coated with a monomolecular layer of a surfactant in a liquid carrier [1–4]. The size of magnetic nanoparticles, MF concentration, and a type of surfactant affect their properties [5,6]. Magnetic fluids have become popular due to a special combination of properties and the ability to change their physical parameters, such as magnetization, sound velocity, and light transmission under the influence of an external magnetic field [7–9].

The interaction between magnetic nanoparticles, the formation and disintegration of aggregates, and changes in physical properties occur in MF under external influences [10–12]. The study of these processes in the MF is difficult since the traditional methods of electron microscopy and atomic force microscopy are carried out under static conditions, while the aggregation process depends on the magnetic fluid dynamics and the magnetic field configuration [13–17]. Viscosity is a physical parameter that is very sensitive to the formation of an internal structure in the MF under the impact of external influences. The change in the viscosity of the MF depending on the strength of the magnetic field (magnetoviscous effect) is one of the most important features of the MF [18,19]. The magnetic field orients the magnetic moment of the particles, complicating their free rotation [20,21]. This causes a local velocity gradient of the base fluid near the particles, which enhances the effective viscosity of the MF [22]. The magnetoviscous effect has been known for a long time; however, recently, research on this topic has received new development due to the spread of microfluidics [23], new data on the formation of structures in magnetic fluids [24–27], the creation of stable magnetorheological fluids [28], and multidisperse systems based on MF with the addition of both magnetic [29] and non-magnetic inclusions [30].

Special mention should be made of bidisperse systems based on MF with the addition of large magnetic particles [31–36]. These systems have colloidal stability, but their viscosity and thermal conductivity significantly change under the influence of an external magnetic

field [37–41]. Such systems are used in dampers [42], acoustic systems [43], seals [44], and sensors [45]. An active element made of ferrofluid oscillates in such systems. However, rotational [25] or capillary viscometry [46] are the main methods for studying the magneto-viscous effect. In this case, aggregates and chain structures are destroyed at high shear rates, as shown in [25]; it is these structures that have the greatest effect on viscosity, according to [24] and the model experiment given in [47].

An alternative method for studying the magnetoviscous effect is the analysis of shear oscillations of a volume of a magnetic fluid levitating in a magnetic field. We found [48–50] that the MF column takes a near-cylindrical shape in a strong magnetic field, transverse to the axis in the tube open on both sides. Hydrodynamic flows are concentrated in a narrow near-wall region during axial oscillations of the liquid column, while the flow of the rest of the liquid is of a piston nature, like the movement of a solid body.

The organization of experiments to study the magnetoviscous effect under conditions of shear oscillations in MFs of fluids with different structures and disperse compositions made it possible to obtain new data on "wall viscosity". The data obtained is important not only for solving technical problems (in which the volume of a magnetic fluid oscillates), but also for studying the mechanisms of rearrangement of the magnetic colloids structure due to the small amplitude of displacement of the sample from the equilibrium position.

2. Materials and Methods

In this work, we used an experimental setup, the scheme of which is shown in Figure 1; it is based on the previously developed method for measuring the viscoelastic parameters of magnetic fluid systems [51–54].

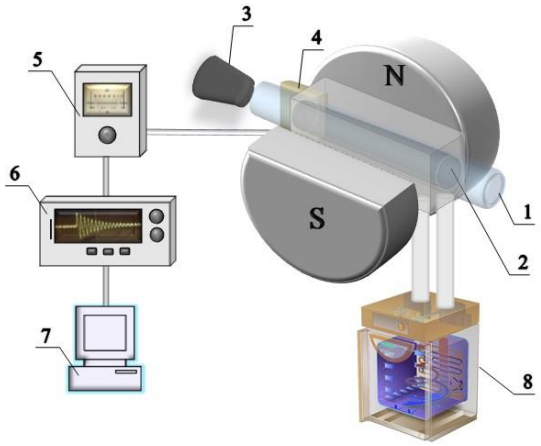


Figure 1. A diagram of the experimental setup.

A FL-1 electromagnet was used during our experiment. A Plexiglas tube (diameter d = 12 mm) 1 is placed between the poles. The tube is filled with magnetic fluid 2 at a field strength of 100 kA/m so that the magnetic fluid is held by the magnetic field and levitates in it. In the initial state, the MF column is equidistant from the centers of the poles. Excitation of oscillations is carried out by piston 3. Inductance coil 4 (5000 turns of copper wire d = 0.071 mm) stands between the tube and the poles of FL-1. The sealed liquid circuit is located around the measuring cell and is connected by a system of silicone flexible tubes to the KRYO-VT-12-1-8 thermostat. The signal from the inductance coil is first amplified using the amplifier 5 of Selective Nanovoltmeter type 237, and then goes to the GwInstek GOS-72074 oscilloscope 6. The resulting waveforms are transferred to computer 7 and processed using the NI Lab-View software. The program calculates frequency and damping factor.

In this work, magnetic fluid was studied; magnetite Fe_3O_4 was used as a base, oleic acid as a stabilizer, and kerosene as a carrier liquid. MF-1, MF-5 samples were manufactured at the Ivanovo State Power Engineering University (ISPU). The MF-3 sample was made at

Southwestern State University (SWSU). MF-1, MF-3, and MF-5 were diluted with kerosene, and MF-2, MF-4, and MF-6 liquids were obtained, respectively. Magnetic fluids MF10–MF-11 were made based on polyethylsiloxane liquid at the ISPU. The physical parameters of the samples are presented in Table 1. The shear viscosity η was measured on a Brookfield DV2T viscometer. The values of MF viscosity in the absence of a magnetic field are given in Table 1 for a spindle speed of 60 rpm, at which the shear rate is 79,2 1/s, which corresponds to the shear rate in the experiment of studying the magnetoviscous effect under conditions of shear oscillations.

Table 1. Physical parameters of MF samples.

Sample	MF Density ρ, kg/m^3	Volume Concentration φ, %	Saturation Magnetization M_s, kA/m	MF Viscosity η, mPa·s
MF-1	1245	11.02	43.3	31.8
MF-2	1058	6.62	20.7	4.15
MF-3	1245	11.06	33	4.05
MF-4	985	4.9	14.7	2.45
MF-5	1382	14.2	49.4	180
MF-6	1080	7.04	23.6	6.3
MF-7	1087	7.22	24.4	5.7
MF-8	1089	7.25	27.4	5.95
MF-9	1091	7.29	31.2	5.5
MF-10	1074	4.78	17	9.45
MF-11	981	2.52	10.03	4.75

The volume concentration of the solid phase φ is determined by the formula:

$$\varphi = \frac{\rho - \rho_f}{\rho_s - \rho_f}, \quad (1)$$

where ρ—is the density of the magnetic fluid, ρ_s—is the density of the magnetite, and ρ_f is the density of the carrier liquid.

The calculated concentration of the solid phase is approximate because it does not take into account the presence of surfactants on magnetic particles.

The magnetization curves for ferrofluid samples are shown in Figure 2. The ballistic method was used to obtain the magnetization curve.

The following experiment was set up to study the dependence of viscosity on concentration: a 10 mL sample of MF-5 was gradually diluted with a small amount of kerosene and its viscosity was measured on a Brookfield DV2T viscometer. The resulting dependence is shown in Figure 3.

From the graph presented in Figure 3, it can be seen that even a small dilution of the original sample causes a significant decrease in its viscosity. The dependence itself is exponential. This course of the graph can be explained by the presence of an excess amount of surfactants, which strongly affects the viscosity of the magnetic fluid. An excess of surfactants is typical for commercial magnetic fluids, which include the MF-5 sample. Similar conclusions were also drawn by the authors in [32,35,46], in which both commercial magnetic fluids and bidisperse systems with the addition of magnetite particles of various sizes were studied. In these works, the authors added large particles without introducing an additional surfactant; this technique was used in our work.

The original MF-5 sample had a significant viscosity and was unsuitable for using in microfluidic systems; therefore, the MF-6 sample was chosen as the basis for obtaining bidisperse systems. Magnetite particles (particle size is 300 nm) were added at a ratio of 1%, 5%, and 10% by weight of the solid phase, and liquid MF-7–MF-9 were obtained, respectively. Fluids were prepared by mechanical and ultrasonic mixing of the magnetite particles with the magnetic fluid.

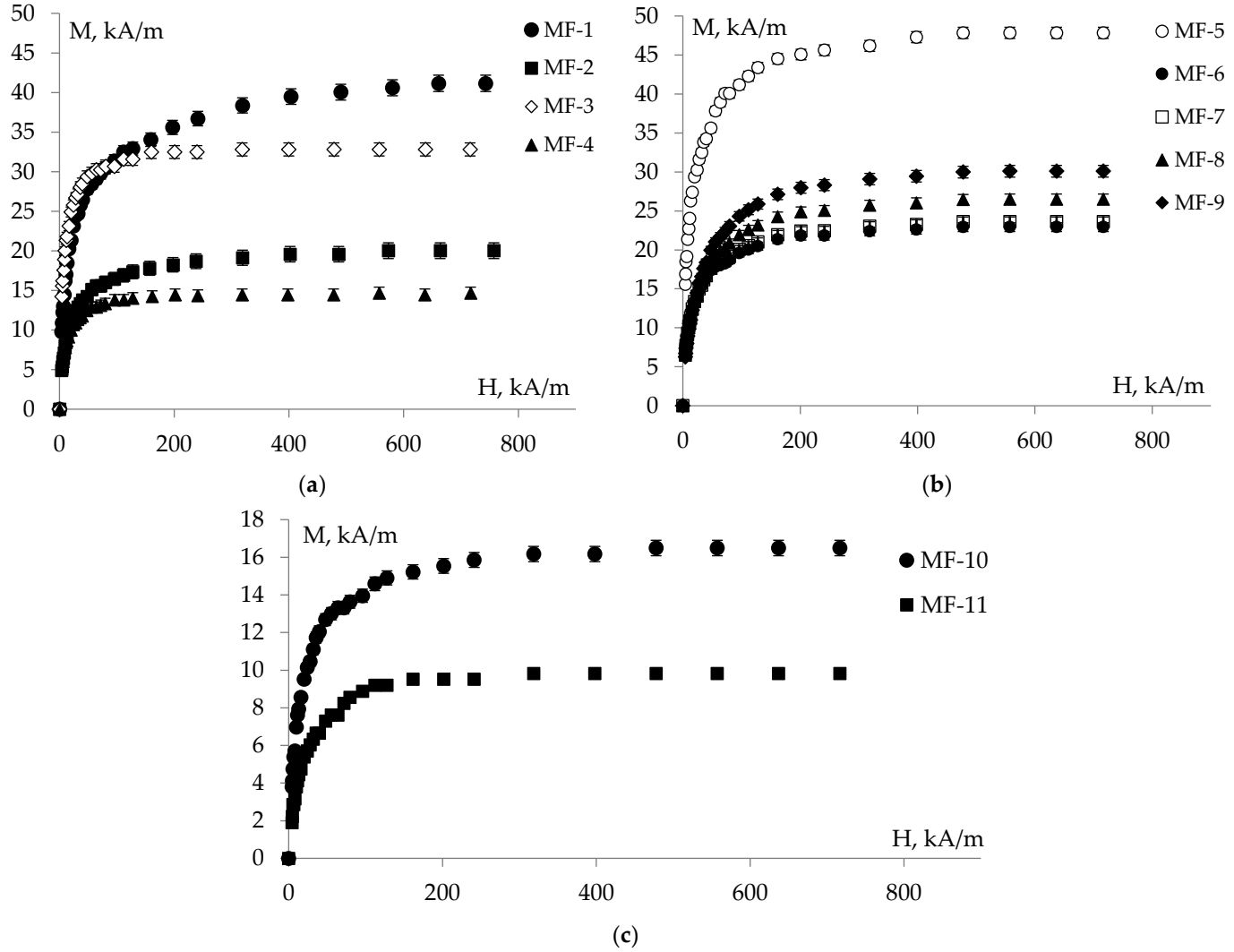


Figure 2. Sample magnetization curves: (**a**) MF-1–MF-4, (**b**) MF-5–MF-9, (**c**) MF-10–MF-11.

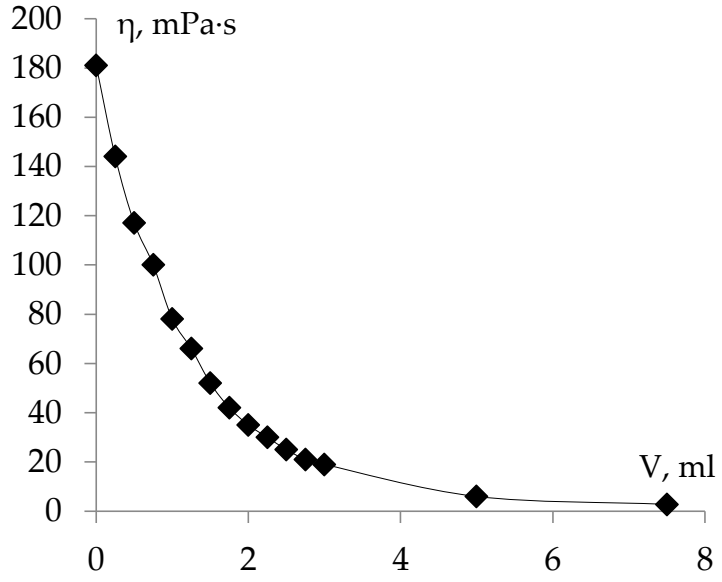
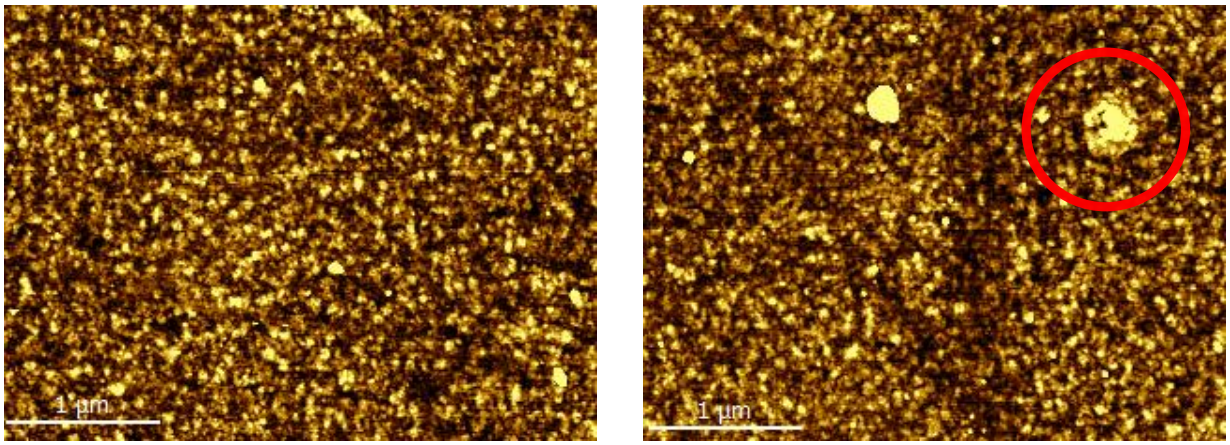


Figure 3. The dependence of the viscosity of MF-5 on dilution with kerosene.

Subsequent analysis showed the absence of delamination and sedimentation in samples MF-7–MF-9. Bidisperse systems turned out to be stable. Table 1 shows the physical parameters of the samples.

Figure 4 shows AFM images for MF-6 and MF-9. AFM images were processed using the Gwyddion data analysis software package. It can be seen that in Figure 4a, particles of standard size are about 20 nm. Figure 4b shows an image showing large inclusions of particles of 200 and 300 nanometers in size. It can be seen from the presented images that there are inclusions of small nanoparticles around large particles, which, in the place with an excess surfactant, form a layer that prevents MF agglomeration (highlighted in a red circle). Such structures were first shown in studies by M. Lopez-Lopez [32], and, in his recent work [34], R. Rosenzweig gave them the definition of "particle clouds".



(**a**) (**b**)

Figure 4. AFM images: (**a**) MF-6, (**b**) MF-9.

3. Results and Discussion

Taking into account the correction for the flow of a viscous fluid, the following expression is given in [51]:

$$\pi^3\nu^2\rho bd^2 + bd\sqrt{\pi^7\nu^3\eta\rho} = \mu_0\frac{\pi d^2}{2}\left(M_x\frac{\partial H_x}{\partial z}\right)_{z=b/2}. \quad (2)$$

where μ_0 is the magnetic permeability, M_x is the field magnetization, $\frac{\partial H_x}{\partial z}$ is the field strength gradient, d is the tube diameter, b is MF column length, ρ is the MF density, η is MF viscosity, ν is MF-column oscillation frequency.

The formula estimating the addition δ_η to the viscous friction of a magnetic fluid in a tube in a shear flow is described in the same paper [51]. It allows for an analysis "from above" (the largest value for a quarter of the period); in this case, the viscous elasticity coefficient k_η is represented as the "average half-period" of the largest value of the harmonic function, namely $k_\eta = 2/\pi \cdot \delta_\eta$. With this in mind:

$$k_\eta = -2bd\sqrt{\pi^5\nu^3\eta_H\rho}. \quad (3)$$

Therefore, expression (2) can be written as:

$$\pi^3\nu^2\rho bd^2 + 2bd\sqrt{\pi^5\nu^3\eta_H\rho} = \mu_0\frac{\pi d^2}{2}\left(M_x\frac{\partial H_x}{\partial z}\right)_{z=b/2}. \quad (4)$$

From this formula we obtain:

$$\eta_H = \frac{1}{\nu^3}\left[\frac{\mu_0 d \cdot M_x}{4b\pi\sqrt{\pi\rho}} \cdot (\partial H_x/\partial z)_{z=b/2} - \frac{\sqrt{\pi\rho} \cdot d \cdot \nu^2}{2}\right]^2. \quad (5)$$

The resulting expression gives an estimate of the MF viscosity in the near-wall layer in the case of shear oscillations of the MF volume in an external magnetic field.

In the expression in parentheses, the minuend is determined by the ponderomotive elasticity of the system, and the subtrahend is determined by the nature of the system's oscillations. Let us write Equation (5) in the form:

$$\eta_H = 1/\nu^3[B - C]^2. \quad (6)$$

where $B = \frac{\mu_0 d \cdot M_x}{4b\pi\sqrt{\pi\rho}} \cdot (\partial H_x/\partial z)_{z=b/2}$, $C = \frac{\sqrt{\pi\rho} \cdot d \cdot \nu^2}{2}$.

Parameter B reflects the magnetic component of the system, and parameter C reflects the elastic component of the system. The dependences of the parameters B and C on the magnetic field strength (Figure 5) were obtained from the data on the gradient of the external magnetic field, the frequency of oscillations, and the geometric dimensions of the MF. In turn, the approximation of these dependencies is shown in the graph; the equations of the approximation lines are presented with errors of less than 1%. The difference between parameters B and C puts significant restrictions on the magnitude of the error when calculating the viscosity; therefore, to obtain the viscosity-magnetic field dependence, approximation equations of straight lines will be used.

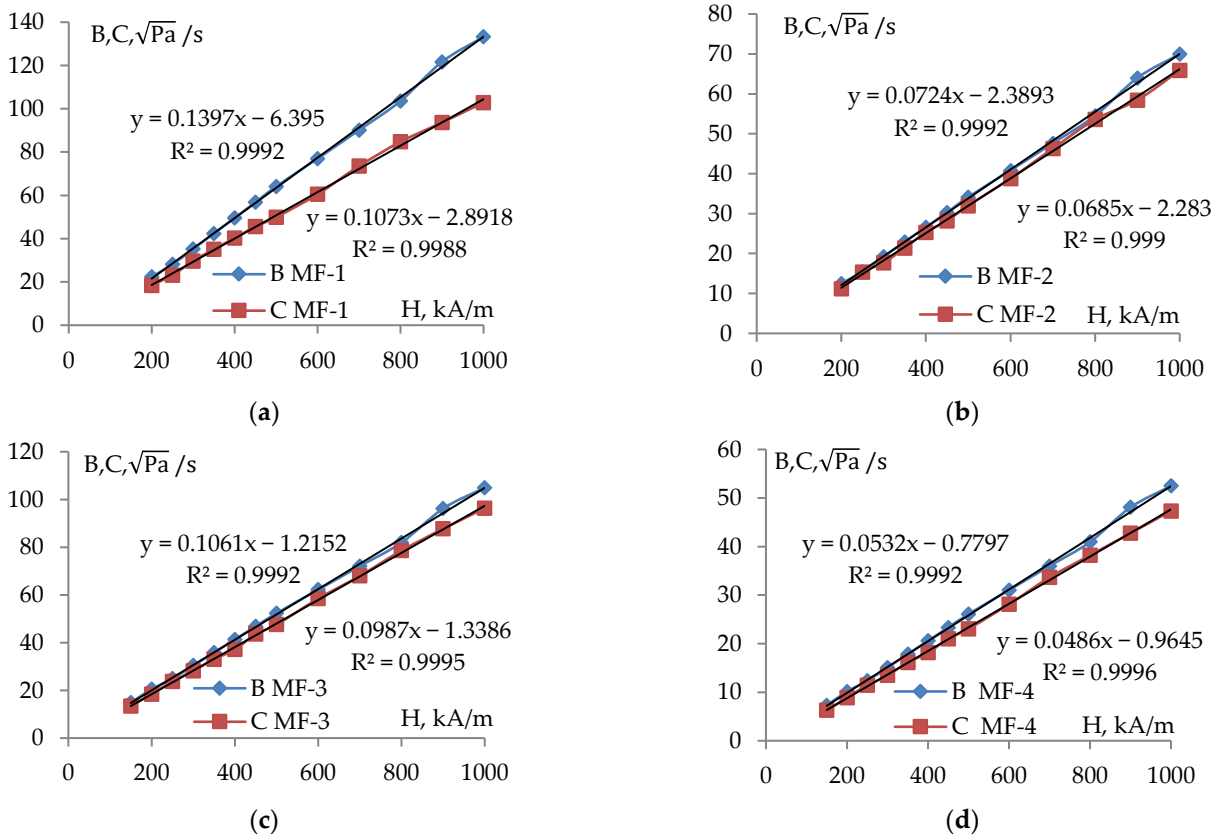


Figure 5. Dependences of parameters B and C: (**a**) MF-1, (**b**) MF-2, (**c**) MF-3, (**d**) MF-4.

The dependences of viscosity for MF-1–MF-4 samples, shown in Figure 6, are built based on the proposed approach. The error in determining the viscosity based on the proposed approach is 10%.

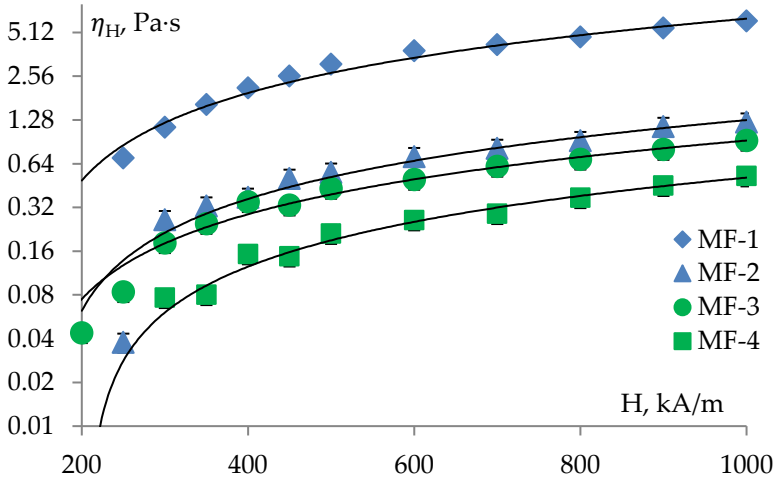


Figure 6. Dependences of viscosity for MF-1–MF-4 samples.

The obtained viscosity dependences show an increase in value by a factor of 5 for the MF-1 sample, with an increase in the field up to 1000 kA/m, which can be explained by interactions between particles and the formation of weakly bound aggregates in the near-wall layer in the more concentrated initial MF-1 sample. Such an increase in viscosity is not observed in the more diluted MF-2 sample. The presence of an excess of free surfactant is typical for samples MF-3 and MF-4, which negatively affects the magnetoviscous effect. The formation of chain structures and aggregates, as shown in [25], may be another reason for the increase in viscosity in a more concentrated MF sample.

A similar effect, as a result of which, during shear flows, microvortices appear in the vicinity of rotating magnetic nanoparticles, which lead to fluid turbulence on a microscopic scale, was first published in [55], where such an effect was observed in an MF with micron-sized aggregates in a rotating horizontal magnetic field.

In the experiment shown in [55], the minimum useful size was measured by the dimer radius of two magnetic nanoparticles $r_0 \cong 14$ nm. This caused a rapid increase in the concentration of magnetic nanoparticles in the boundary layer up to $\alpha \sim 0,5$ and, as a consequence, an increase in near-wall viscosity. The conclusions presented in [55] confirmed the assumption made that the increase in viscosity in a magnetic field when exposed to the interfacial boundaries of a levitating MF column can be explained by an increase in particle interactions, which lead to MF microstructuring in the near-wall layer.

The dependence of the viscosity of samples MF-6–MF-9 according to the proposed method is shown in Figure 7.

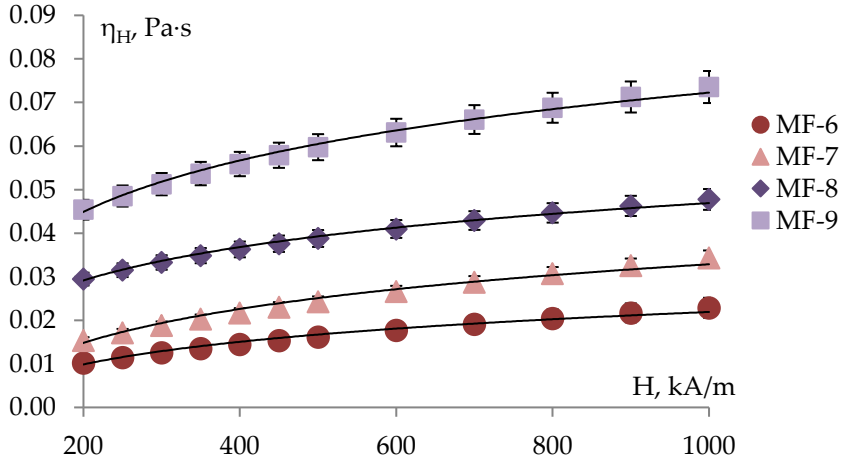


Figure 7. Dependence of viscosity on magnetic field strength for samples MF-6–MF-9.

The obtained dependences of viscosity for MF-6–MF-9 show an increase in the viscosity value depending on the number of iron particles contained in the ferrofluid. The more content of the mass fraction of large particles of magnetite, the higher the viscosity in the near-wall layer.

As the concentration of magnetic nanoparticles in the magnetic fluid increases, the bonds between the particles become stronger, and the near-wall viscosity increases.

The dependence of viscosity on temperature is another important characteristic of these systems. During the experiment, the required temperature was set in the measuring cell, which was maintained for 10–20 min to stabilize the system, and then the frequency and attenuation coefficient were measured by changing the magnetic field strength.

We use the Helmholtz formula to analyze the viscosity of a ferrofluid:

$$\eta_H = \frac{\beta^2 d^2 \rho}{4\pi\nu}. \quad (7)$$

Dependences of ferrofluid viscosity on magnetic field strength and temperature for MF-10–MF-11 are shown in Figures 8 and 9.

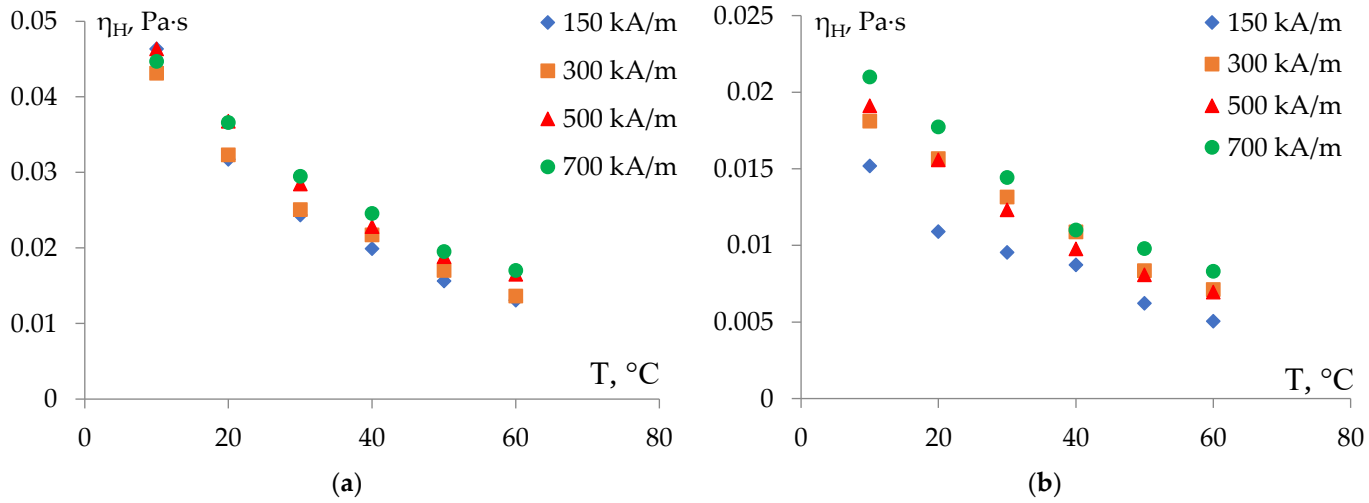


Figure 8. Dependence of the ferrofluid viscosity on temperature: (**a**) MF-10, (**b**) MF-11.

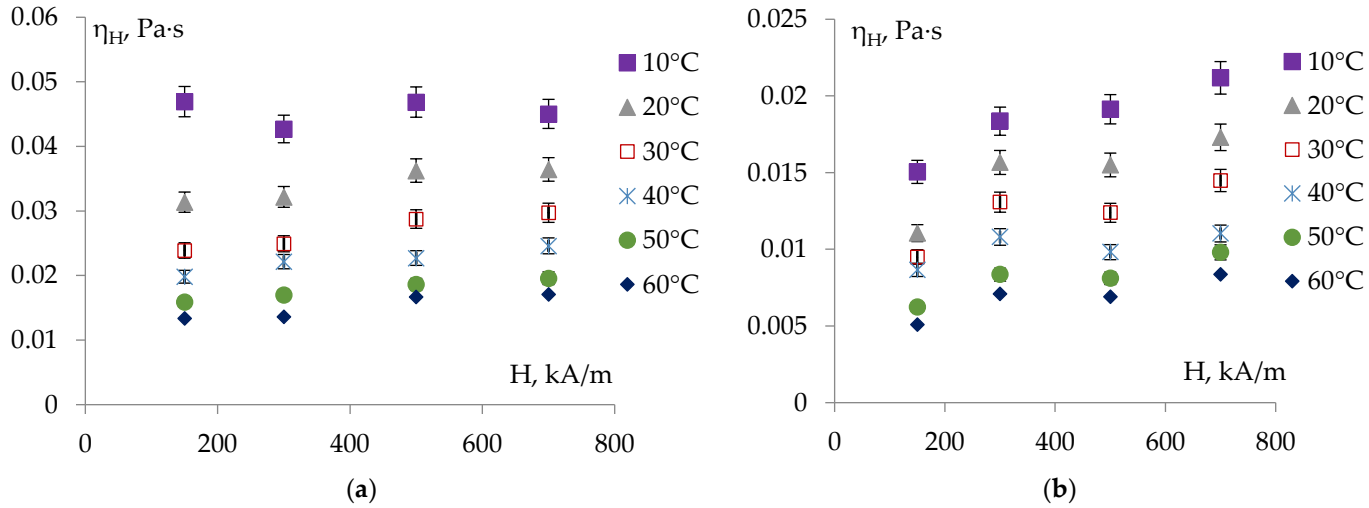


Figure 9. Dependence of the magnetic fluid viscosity on the magnetic field strength: (**a**) MF-10, (**b**) MF-11.

The given estimate of the magnetic fluid viscosity is qualitative and cannot be used for a rigorous description, since the magnetic fluid is non-Newtonian, and the expression for the Helmholtz viscosity is suitable for Newtonian fluids. These plots show a trend towards increasing viscosity with increasing magnetic field strength and decreasing with increasing temperature.

4. Conclusions

This study considered the magnetoviscous effect under the conditions of shear vibrations in MF samples with different structures, manufacturing technology, carrier liquids, and surfactant concentrations. Images of bidisperse systems based on magnetic fluid with the addition of various concentrations of large magnetic particles were also studied. Two methods for determining the viscosity of the MF were proposed in the work: the first one was based on measuring the frequency of oscillations of the MF levitating volume (Formulas (5) and (6)), the second one was based on the Helmholtz Formula (7). The increase in viscosity for the concentrated colloid MF-1 was five times, with an increase in the magnetic field strength up to 1000 kA/m. This dependence can be explained by the formation of chain structures and aggregates, which coincides with the estimates in [24,25]. The increase in viscosity in the diluted MF-2 sample coincides with the data of [18]. The negative effect of an excess in surfactants on the magnetoviscous effect was established in the work. The increase in viscosity in a magnetic field for such samples (MF-3, MF-4) was less than in standard MF samples. However, an excess of surfactants made it possible to create stable bidisperse systems based on MF with the addition of large magnetic particles. Similar systems were obtained in [32,46]. The formation of stable structures of "particle clouds" was established by AFM microscopy (Figure 3). These structures were first described in [32,34]. A large magnetic particle was located in the center of the "cloud", and its surface was covered with small nanoparticles. An experiment to study the magnetoviscous effect in shear vibrations in bidisperse systems was carried out. The work (Figure 7) shows that an increase in viscosity is directly proportional to the concentration of large magnetic particles, which coincides with the data of [34]; however, the increase in viscosity is larger, which can be explained by the formation of structures in the near-wall layer, as shown in [24,25,47]. Based on the Helmholtz Formula (7), data were obtained on the dependence of the magnetoviscous effect on temperature in shear vibrations. In this experiment, viscosity was inversely proportional to temperature. The results obtained can be used in the development of express tests of magnetic fluid samples and the creation of acceleration and vibration sensors. The results of this paper can also be used to study the agglomeration of nanoparticles. Information on the magnetic-viscous effect in a thin near-wall layer under conditions of shear oscillations will be valuable for microfluidic technologies, where magnetic fluids and bidisperse systems based on them are used in channels of various shapes.

Author Contributions: Conceptualization, E.S. and P.R.; methodology, E.S. and P.R.; software, P.R.; validation, E.S., P.R. and A.C.; formal analysis, E.S.; investigation, E.S.; resources, A.C.; data curation, E.S. and P.R.; writing—original draft preparation, E.S.; writing—review and editing, P.R.; visualization, E.S.; supervision, P.R.; project administration, P.R.; funding acquisition, P.R. All authors have read and agreed to the published version of the manuscript.

Funding: This research was funded by the part of the implementation of the Russian Federation State task (No 0851-2020-0035) and as the part of the implementation of the program of strategic academic leadership "Priority-2030" (Agreements No. 075-15-2021-1155 and No. 075-15-2021-1213).

Data Availability Statement: The data presented in this study are available on request from the corresponding author. The data are not publicly available due to privacy.

Conflicts of Interest: The authors declare no conflict of interest.

References

1. Rosensweig, R.E. *Ferrohydrodynamics*; Courier Corporation: Chelmsford, MA, USA, 2013; 368p.
2. Socoliuc, V.; Avdeev, M.V.; Kuncser, V.; Turcu, R.; Tombácz, E.; Vekas, L. Ferrofluids and bio-ferrofluids: Looking back and stepping forward. *Nanoscale* **2022**, *14*, 4786–4886. [CrossRef]
3. Zhang, X.; Sun, L.; Yu, Y.; Zhao, Y. Flexible ferrofluids: Design and applications. *Adv. Mater.* **2019**, *31*, 1903497. [CrossRef] [PubMed]
4. Odenbach, S. *Colloidal Magnetic Fluids: Basics, Development and Application of Ferrofluids*; Lecture Notes in Physics; Springer: Berlin/Heidelberg, Germany, 2009; Volume 763, 429p. [CrossRef]
5. Philip, J. Magnetic nanofluids: Recent advances, applications, challenges, and future directions. *Adv. Colloid Interface Sci.* **2022**, *311*, 102810. [CrossRef] [PubMed]
6. Huang, C.; Yao, J.; Zhang, T.; Chen, Y.; Jiang, H.; Li, D. Damping applications of ferrofluids: A review. *J. Magn.* **2017**, *22*, 109–121. [CrossRef]
7. Lebedev, A.V.; Kantorovich, S.S.; Ivanov, A.O.; Arefyev, I.M.; Pshenichnikov, A.F. Weakening of magnetic response experimentally observed for ferrofluids with strongly interacting magnetic nanoparticles. *J. Mol. Liq.* **2019**, *277*, 762–768. [CrossRef]
8. Bashtovoi, V.; Reks, A.; Kuzhir, P.; Zubarev, A.; Volkova, O.; Moroz, V. Effect of magnetophoresis and Brownian diffusion on mechanical processes in magnetic fluids: The role of a condensation phase transition. *J. Magn. Magn. Mater.* **2020**, *498*, 166148. [CrossRef]
9. Polunin, V.M.; Tantsyura, A.O.; Storozhenko, A.M.; Ryapolov, P.A. Study of demagnetizing field induced by a sound wave. *Acoust. Phys.* **2013**, *59*, 662–666. [CrossRef]
10. Zakinyan, A.A.; Belykh, S.S.; Zakinyan, A.R.; Yerin, K.V. Structured media based on magnetic colloids as a promising material for magnetically controllable optical elements. *J. Opt. Technol.* **2021**, *88*, 158–165. [CrossRef]
11. Ivanov, A.S.; Pshenichnikov, A.F. Magnetostatic buoyancy force acting on a non-magnetic sphere immersed in a ferrofluid magnetized by a gradient field. *J. Magn. Magn. Mater.* **2022**, *565*, 170294. [CrossRef]
12. Ivanov, A.S.; Solovyova, A.Y.; Zverev, V.S.; Elfimova, E.A. Distribution functions of magnetic moments and relaxation times for magnetic fluids exhibiting controllable microstructure evolution. *J. Mol. Liq.* **2022**, *367*, 120550. [CrossRef]
13. Lacava, L.M.; Lacava, B.M.; Azevedo, R.B.; Lacava, Z.G.M.; Buske, N.; Tronconi, A.L.; Morais, P.C. Nanoparticle sizing: A comparative study using atomic force microscopy, transmission electron microscopy, and ferromagnetic resonance. *J. Magn. Magn. Mater.* **2001**, *225*, 79–83. [CrossRef]
14. Passeri, D.; Angeloni, L.; Rossi, M. *Magnetic Force Microscopy and Magnetic Nanoparticles: Perspectives and Challenges*; In New Trends in Nanoparticle Magnetism; Springer: Cham, Switzerland, 2021; Volume 308, pp. 285–300. [CrossRef]
15. Raşa, M.; Kuipers, B.W.M.; Philipse, A.P. Atomic force microscopy and magnetic force microscopy study of model colloids. *J. Colloid Interface Sci.* **2002**, *250*, 303–315. [CrossRef] [PubMed]
16. Butter, K.; Bomans, P.H.H.; Frederik, P.M.; Vroege, G.J.; Philipse, A.P. Direct observation of dipolar chains in iron ferrofluids by cryogenic electron microscopy. *Nat. Mater.* **2003**, *2*, 88–91. [CrossRef] [PubMed]
17. Butter, K.; Bomans, P.H.; Frederik, P.M.; Vroege, G.J.; Philipse, A.P. Direct observation of dipolar chains in ferrofluids in zero field using cryogenic electron microscopy. *J. Phys. Condens. Matter* **2003**, *15*, S1451. [CrossRef]
18. Morillas, J.R.; de Vicente, J. Magnetorheology: A review. *Soft Matter* **2020**, *16*, 9614–9642. [CrossRef]
19. Damdinov, B.B.; Mitypov, C.M.; Ershov, A.A.; An, V.V. Bulk Viscosity in Liquids and Liquid Disperse Systems. *Russ. Phys. J.* **2022**, *65*, 840–846. [CrossRef]
20. Odenbach, S. Magnetic fluids-suspensions of magnetic dipoles and their magnetic control. *J. Phys. Condens. Matter* **2003**, *15*, S1497. [CrossRef]
21. El-Sapa, S. The force on a magneto-spherical particle oscillating in a viscous fluid perpendicular to an impermeable planar wall with slippage. *European J. Pure Appl. Math.* **2022**, *15*, 1376–1401. [CrossRef]
22. Afifah, A.N.; Syahrullail, S.; Sidik, N.A.C. Magnetoviscous effect and thermomagnetic convection of magnetic fluid: A review. *Renew. Sustain. Energy Rev.* **2016**, *55*, 1030–1040. [CrossRef]
23. Nam-Trung, N. Micro-magnetofluidics: Interactions between magnetism and fluid flow on the microscale. *Microfluid. Nanofluid* **2012**, *12*, 1–16. [CrossRef]
24. Ivanov, A.O.; Zubarev, A. Chain formation and phase separation in ferrofluids: The influence on viscous properties. *Materials* **2020**, *13*, 3956. [CrossRef] [PubMed]
25. Mishra, A.; Pathak, S.; Kumar, P.; Singh, A.; Jain, K.; Chaturvedi, R.; Pant, R.P. Measurement of static and dynamic magneto-viscoelasticity in facile varying pH synthesized $CoFe_2O_4$-based magnetic fluid. *IEEE Trans. Magn.* **2019**, *55*, 1–7. [CrossRef]
26. Pathak, S.; Verma, R.; Kumar, P.; Singh, A.; Singhal, S.; Sharma, P.; Wang, X. Facile synthesis, static, and dynamic magnetic characteristics of varying size double-surfactant-coated mesoscopic magnetic nanoparticles dispersed stable aqueous magnetic fluids. *Nanomaterials* **2021**, *11*, 3009. [CrossRef] [PubMed]
27. Kumar, P.; Pathak, S.; Singh, A.; Khanduri, H.; Wang, X.; Basheed, G.A.; Pant, R.P. Optimization of cobalt concentration for improved magnetic characteristics and stability of $Co_xFe_{3-x}O_4$ mixed ferrite nanomagnetic fluids. *Mater. Chem. Phys.* **2021**, *265*, 124476. [CrossRef]
28. Shahrivar, K.; Morillas, J.R.; Luengo, Y.; Gavilan, H.; Morales, P.; Bierwisch, C.; de Vicente, J. Rheological behavior of magnetic colloids in the borderline between ferrofluids and magnetorheological fluids. *J. Rheol.* **2019**, *63*, 547–558. [CrossRef]

29. Shah, K.; Choi, S.B. The influence of particle size on the rheological properties of plate-like iron particle based magnetorheological fluids. *Smart Mater. Struct.* **2014**, *24*, 015004. [CrossRef]
30. Liu, X.; Li, D. Tuning the magneto-rheological properties of magnetic fluid using hydrophilic fumed silica nanoparticles. *Soft Matter* **2021**, *17*, 8175–8184. [CrossRef]
31. Jain, K.; Kumar, P.; Pant, R.P.; Basheed, G.A. Tunning of rheological and magnetic properties of Ni doped magnetite based magnetic nanofluid. *Phys. B Condens. Matter* **2022**, *643*, 414136. [CrossRef]
32. López-López, M.T.; De Vicente, J.; Bossis, G.; González-Caballero, F.; Durán, J.D.G. Preparation of stable magnetorheological fluids based on extremely bimodal iron–magnetite suspensions. *J. Mater. Res.* **2005**, *20*, 874–881. [CrossRef]
33. Cvek, M.; Jamatia, T.; Suly, P.; Urbanek, M.; Torres-Mendieta, R. Stable Magnetorheological Fluids Containing Bidisperse Fillers with Compact/Mesoporous Silica Coatings. *Int. J. Mol. Sci.* **2022**, *23*, 11044. [CrossRef]
34. Rosensweig, R.E. Magnetorheological particle clouds. *J. Magn. Magn. Mater.* **2019**, *479*, 301–306. [CrossRef]
35. Susan-Resiga, D.; Socoliuc, V.; Bunge, A.; Turcu, R.; Vékás, L. From high colloidal stability ferrofluids to magnetorheological fluids: Tuning the flow behavior by magnetite nanoclusters. *Smart Mater. Struct.* **2019**, *28*, 115014. [CrossRef]
36. Siebert, E.; Dupuis, V.; Neveu, S.; Odenbach, S. Rheological investigations on the theoretical predicted "Poisoning" effect in bidisperse ferrofluids. *J. Magn. Magn. Mater.* **2015**, *374*, 44–49. [CrossRef]
37. Susan-Resiga, D.; Vékás, L. Yield stress and flow behavior of concentrated ferrofluid-based magnetorheological fluids: The influence of composition. *Rheol. Acta* **2014**, *53*, 645–653. [CrossRef]
38. Doganay, S.; Alsangur, R.; Turgut, A. Effect of external magnetic field on thermal conductivity and viscosity of magnetic nanofluids: A review. *Mater. Res. Express* **2019**, *6*, 112003. [CrossRef]
39. Pathak, S.; Jain, K.; Kumar, P.; Wang, X.; Pant, R.P. Improved thermal performance of annular fin-shell tube storage system using magnetic fluid. *Appl. Energy* **2019**, *239*, 1524–1535. [CrossRef]
40. Iwamoto, Y.; Kondoh, S.; Ido, Y.; Yamamoto, H.; Nishida, H.; Yamasaki, H.; Jeyadevan, B. Influence of size on anisotropic thermophysical properties of magnetic suspensions. *Int. J. Appl. Electromagn. Mech.* **2018**, *58*, 371–385. [CrossRef]
41. Lei, J.; Luo, Z.; Qing, S.; Huang, X.; Li, F. Effect of surfactants on the stability, rheological properties, and thermal conductivity of Fe3O4 nanofluids. *Powder Technol.* **2022**, *399*, 117197. [CrossRef]
42. Li, Y.; Han, P.; Li, D.; Chen, S.; Wang, Y. Typical dampers and energy harvesters based on characteristics of ferrofluids. *Friction* **2022**, *11*, 165–186. [CrossRef]
43. Purnomo, E.D.; Ubaidillah, U.; Imaduddin, F.; Yahya, I.; Mazlan, S.A. Preliminary experimental evaluation of a novel loud-speaker featuring magnetorheological fluid surround absorber. *Indones. J. Electr. Eng. Comput. Sci.* **2020**, *17*, 922–928. [CrossRef]
44. Li, Z.; Li, D. A comparative study of magnetic seals by ferrofluids, magnetorheological fluids and magnetic powders. *Front. Mater.* **2022**, *9*, 984761. [CrossRef]
45. Yao, J.; Liu, J.; Hu, Y.; Li, Z.; Li, D. The Theoretical and Experimental Study of a Ferrofluid Inertial Sensor. *IEEE Sens. J.* **2021**, *22*, 107–114. [CrossRef]
46. Nowak, J.; Borin, D.; Haefner, S.; Richter, A.; Odenbach, S. Magnetoviscous effect in ferrofluids diluted with sheep blood. *J. Magn. Magn. Mater.* **2017**, *442*, 383–390. [CrossRef]
47. Huang, H.; Li, H.; Wang, W.; Peng, X. Analysis on the enhancement mechanism of bidisperse magnetorheological fluid based on the local microstructural models. *Rheol. Acta* **2022**, *61*, 87–98. [CrossRef]
48. Polunin, V.M.; Ryapolov, P.A.; Zhakin, A.I.; Ivanov, A.M.; Shel'deshova, E.V. Magnetoviscous effect in case of magnetic fluid oscillations in strong magnetic field. *Magnetohydrodynamics* **2018**, *54*, 353–360.
49. Karpova, G.V.; Kutuev, A.N.; Ryapolov, P.A.; Polunin, V.M.; Zubarev, E.K.; Kovarda, V.V. On the dissipation processes in the oscillating system with a magneto-liquid element. *Magnetohydrodynamics* **2009**, *45*, 85–93.
50. Polunin, V.M.; Ryapolov, P.A.; Platonov, V.B.; Kuz'ko, A.E. Free oscillations of magnetic fluid in strong magnetic field. *Acoust. Phys.* **2016**, *62*, 313–318. [CrossRef]
51. Polunin, V.M.; Ryapolov, P.A.; Shel'deshova, E.V.; Kuz'ko, A.E.; Aref'ev, I.M. Dynamic Elasticity of a magnetic fluid column in a strong magnetic field. *Russ. Phys. J.* **2017**, *60*, 381–388. [CrossRef]
52. Ryapolov, P.A.; Polunin, V.M.; Shel'deshova, E.V. An alternative way to study magnetic fluid magnetization and viscosity. *J. Magn. Magn. Mater.* **2020**, *496*, 165924. [CrossRef]
53. Polunin, V.M.; Ryapolov, P.A.; Zhakin, A.I.; Sheldeshova, E.V. Viscosity of a Magnetic Fluid in a Strong Magnetic Field. *Acoust. Phys.* **2019**, *65*, 379–384. [CrossRef]
54. Polunin, V.M.; Ryapolov, P.A.; Platonov, V.B.; Sheldeshova, E.V.; Karpova, G.V.; Aref'ev, I.M. Elasticity of a magnetic fluid in a strong magnetic field. *Acoust. Phys.* **2017**, *63*, 416–423. [CrossRef]
55. Leupold, H.A.; Tilak, A.S.; Potenziani, E. Multi-Tesla permanent magnet field sources. *J. Appl. Phys.* **1993**, *73*, 6861–6863. [CrossRef]

Disclaimer/Publisher's Note: The statements, opinions and data contained in all publications are solely those of the individual author(s) and contributor(s) and not of MDPI and/or the editor(s). MDPI and/or the editor(s) disclaim responsibility for any injury to people or property resulting from any ideas, methods, instructions or products referred to in the content.